Density of photon states in dye-doped chiral nematic liquid crystal cells in the presence of losses and gain

Density of photon states in dye-doped chiral nematic liquid crystal cells in the presence of losses and gain

Th. K. Mavrogordatos, S. M. Morris, F. Castles, P. J. W. Hands, A. D. Ford, H. J. Coles, and T. D. Wilkinson*
Centre of Molecular Materials for Photonics and Electronics, Department of Engineering, University of Cambridge, 9 JJ Thomson Avenue, Cambridge CB3 0FA, United Kingdom
(Received 17 February 2012; published 12 July 2012)

We calculate the density of photon states (DOS) of the normal modes in dye-doped chiral nematic liquid crystal (LC) cells in the presence of various loss mechanisms. Losses and gain are incorporated into the transmission characteristics through the introduction of a small imaginary part in the dielectric constant perpendicular and along the director, for which we assume no frequency dispersion. Theoretical results are presented on the DOS in the region of the photonic band gap for a range of values of the loss coefficient and different values of the optical anisotropy. The obtained values of the DOS at the photonic band gap edges predict a reversal of the dominant modes in the structure. Our results are found to be in good agreement with the experimentally obtained excitation thresholds in chiral nematic LC lasers. The behavior of the DOS is also discussed for amplifying LC cells providing additional insight to the lasing mechanism of these structures.

DOI: 10.1103/PhysRevE.86.011705 PACS number(s): 42.70.Df, 42.70.Hj

Photonic band edge lasing has been extensively demonstrated in dye-doped chiral nematic liquid crystal (LC) cells [1,2]. Feedback is provided by the modulation of the refractive index as the director precesses continually and orthogonally along the optical axis forming a helical structure with pitch p. Optical gain, on the other hand, is provided through the addition of a gain medium such as a laser dye. In recent years, these lasers have attracted interest because of their remarkable emission characteristics in the form of broadband wavelength tunability, narrow linewidth emission, and high slope efficiencies [2–4].

The observed lasing behavior near the edges of the photonic band gap can be explained by the drastic changes in the density of photon states (DOS). Divergence in the DOS at the band edges in chiral nematic LCs was shown theoretically and experimentally by Schmidtke *et al.* [5] who considered the fluorescence characteristics from a dye-doped chiral nematic LC in the region of the photonic band gap. Subsequently, for laser emission it has been shown that, in analyzing the case of a Fabry-Perot (FP) resonator, the threshold gain g_{th} can be related directly to the DOS ρ as [3]

$$g_{\mathrm{th}} \propto \frac{n_{\mathrm{r}}}{L\rho}, \tag{1}$$

where n_{r} is the real part of the refractive index inside a resonator of length L. In Eq. (1), ρ is the maximum DOS in the resonator when only loss mechanisms are considered, apart from stimulated absorption [3]. Furthermore, according to the space-independent rate equations the slope efficiency can be shown to be inversely proportional to the threshold energy and therefore directly proportional to ρ [6].

Losses will be important in the design of optimized practical systems: they will affect the DOS and hence the threshold gain and the slope efficiency. Blinov recently considered the effect of losses on the threshold gain of a LC laser by incorporating a simple correction factor *a posteriori* [7]. In this paper we calculate the effect of losses and gain directly on the DOS. This is achieved by building upon the analysis of Schmidtke *et al.* [5] and de Vries [8] for a lossless system, which we modify to include imaginary parts in the parallel and perpendicular dielectric coefficients. We will show that small losses have appreciable and unexpected effects on the DOS, such as a reversal of the dominant edge mode, and hence also on the threshold gain. The modified DOS is investigated for various cell thicknesses and optical anisotropies. We then correlate our theoretical results with experimentally determined excitation thresholds, finding good agreement. Finally, the behavior of the DOS corresponding to stimulated emission close to the lasing threshold condition is discussed.

To introduce losses into the transmission coefficient it is first necessary to construct a formulation for the DOS in terms of the transmission coefficient. For a light wave propagating along the helix of a chiral nematic LC film there are two eigenmodes corresponding to elliptically polarized plane waves with an opposite sense of rotation. Their polarization is wavelength dependent [5,8]. The probability of photon emission by an excited fluorescent molecule, as obtained by Fermi's golden rule [5,9], is the product of the DOS and the square of the matrix elements corresponding to the coupling of the electric field with the electric dipole moment of the gain medium. Hence the relative intensity contributions of the two eigenmodes can be written as [5]

$$I_j = \frac{|\rho_j| \int_0^L \langle |E_j^* \cdot \hat{d}|\rangle^2 dz}{|\rho_{\mathrm{iso}}| \int_0^L \langle |E_{\mathrm{iso}}^* \cdot \hat{d}|\rangle^2 dz}, \quad j = 1,2, \tag{2}$$

where ρ_j is the DOS for the jth eigenmode, E_j is the corresponding eigenfield, and $\hat{d}$ is the normalized dipole moment. In Eq. (2), the average of the orientational distribution of the dipole moment across the LC cell with length L is calculated and normalized to an expression with the intensity contribution of the fluorescent dye molecules incorporated into an isotropic medium. For a transmission coefficient of the structure written in the form $T_j(\omega) = X_j(\omega) + iY_j(\omega), j =$

*Author to whom correspondence should be addressed: tdw13@cam.ac.uk

1,2, the DOS then becomes [5,10]

$$\rho_j = \frac{1}{L}\frac{\frac{dY_j}{d\omega}X_j - \frac{dX_j}{d\omega}Y_j}{X_j^2 + Y_j^2}, \quad j = 1,2, \tag{3}$$

and for the isotropic case $\rho_{\rm iso}$ is independent of the frequency ($\rho_{\rm iso} = n/c$, where n is the refractive index and c is the speed of light in the vacuum). For a nonabsorbing medium, expressions for X_j and Y_j can be found in Ref. [5] for the transmission coefficient of the chiral nematic LC structure.

In order to calculate the transmission properties of the helical structure it is useful to define the relative dielectric anisotropy at optical frequencies as $\alpha = (\varepsilon_\parallel - \varepsilon_\perp)/(\varepsilon_\parallel + \varepsilon_\perp)$ and the reduced wavelength $\lambda' = \lambda/(np) \equiv (\sqrt{2}\lambda)/(p\sqrt{\varepsilon_\parallel + \varepsilon_\perp})$ which are both dimensionless ($\varepsilon_\perp$and $\varepsilon_\parallel$ are the relative dielectric constants perpendicular and parallel to the director, respectively) as proposed by de Vries [8]. Without loss of generality we may assume that $p > 0$ which corresponds to a right-handed helical structure [5]. The dielectric anisotropy at optical frequencies is an alternative measure of the birefringence of the LC host and an implicit indication of feedback strength in an analogous way to the mirror reflectivities in a FP resonator.

When considering absorption in a dye-doped LC laser configuration we must keep in mind that the same host is an absorbing medium for the pump beam and simultaneously for the spontaneous emission of the fluorescent dyes. For the dye emission (as well as for the pumping beam propagation inside the active medium), one has to take into account various loss mechanisms including linear absorption, light scattering from imperfections, cavity losses due to light escaping from the cavity, and Förster resonance energy transfer when two chromophores are involved [3]. While spontaneous emission is considered as randomly polarized, we assume that fluorescence is coupled to a particular normal mode with specific polarization properties in the presence of a chiral nematic LC medium. Both losses and gain can be incorporated into our analysis through introducing a small imaginary part to the dielectric constants parallel and perpendicular to the director, as $\gamma_\perp$ and $\gamma_\parallel$, respectively, altogether amassed to the dimensionless constant $\gamma = \gamma_\perp + \gamma_\parallel$ for which we assume no frequency dispersion and $|\gamma| \ll 1$ following a similar treatment as in [11].

For a complex dielectric constant, the transmission coefficient for the diffracting eigenwave is then modified to (for simplicity we will drop the suffix, $j = 1$)

$$T \propto A(m,\lambda)\frac{\exp(ikNp)}{1 - r^2\exp(2ikNp)} = A(m,\lambda)T'(\lambda,m,N), \tag{4}$$

with

$$k = k_a(\lambda) + ik_b(\lambda) = \frac{2\pi m}{\lambda}, \tag{5}$$

and

$$r = r_a(\lambda) + ir_b(\lambda) = -\frac{n - (\lambda/p)f - m}{n + (\lambda/p)f + m}, \tag{6}$$

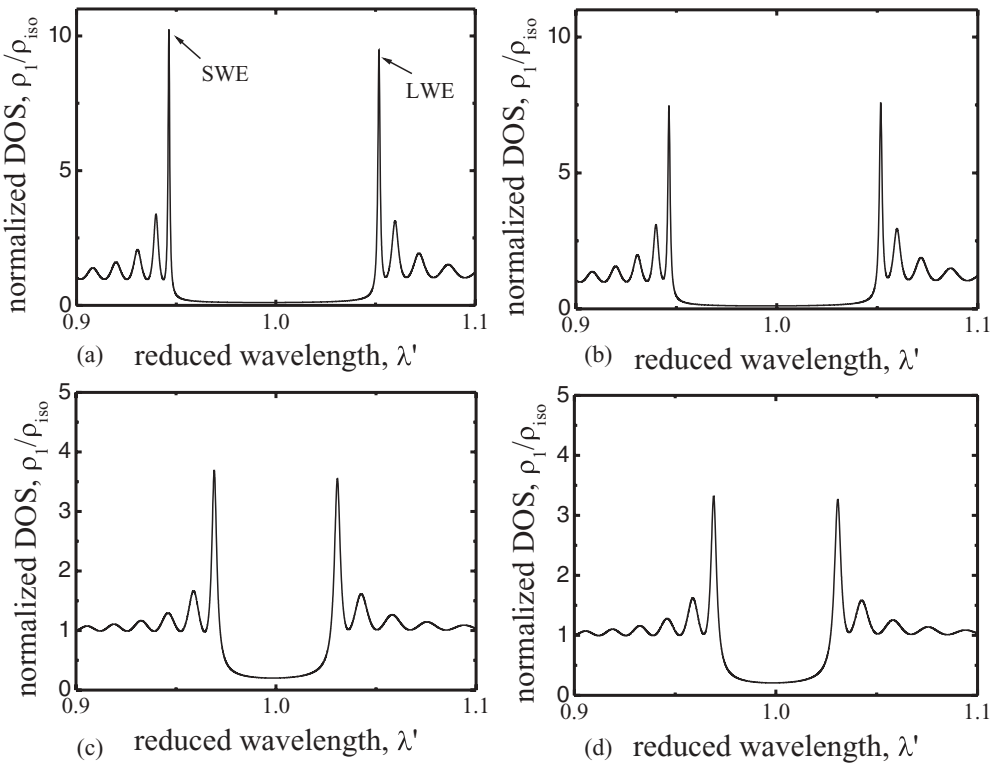

FIG. 1. Theoretical results of the normalized DOS of the eigenwave E_1 ($\rho_1/\rho_{\rm iso}$) for a chiral nematic cell as a function of reduced wavelength for different values of the loss coefficient and the optical anisotropy. For all plots, the cell thickness was fixed at $L = 30p$. (a) $n = 1.581$ relative dielectric anisotropy at optical frequencies, $\alpha = 0.1$ loss coefficient $\gamma = 2\gamma_\parallel = 0.0002$, (b) $n = 1.581$, $\alpha = 0.1$ loss coefficient $\gamma = 2\gamma_\parallel = 0.002$, (c) $n = 1.541$, $\alpha = 0.0526$ and loss coefficient $\gamma = 2\gamma_\parallel = 0.0002$ and (d) $n = 1.541$, $\alpha = 0.0526$ loss coefficient $\gamma = 2\gamma_\parallel = 0.002$.

with

$$f = \frac{\lambda p\left[\frac{\varepsilon_\perp + i\gamma_\perp}{\lambda^2} - \frac{1}{p^2} - \left(\frac{m}{\lambda}\right)^2\right]}{2m} = \frac{2m}{\lambda p\left[\frac{\varepsilon_\parallel + i\gamma_\parallel}{\lambda^2} - \frac{1}{p^2} - \left(\frac{m}{\lambda}\right)^2\right]}. \tag{7}$$

In the above relations, the modified "refractive index" m is the solution of the equation [8]

$$m^4 - m^2\left[\varepsilon_\perp + \varepsilon_\parallel + i\gamma + 2\left(\frac{\lambda}{p}\right)^2\right] + \left[\varepsilon_\perp + i\gamma_\perp - \left(\frac{\lambda}{p}\right)^2\right] \times \left[\varepsilon_\parallel + i\gamma_\parallel - \left(\frac{\lambda}{p}\right)^2\right] = 0, \tag{8}$$

which corresponds to the diffracting eigenwave.

The real and imaginary parts of $T'(\lambda,m,N)$ can be written as

$$X' = -\cos(k_a Np)r_a^2 + 2r_a r_b \sin(k_a Np) + \cos(k_a Np)r_b^2 + \exp(2k_b Np)\cos(k_a Np), \tag{9a}$$

and

$$Y' = \sin(k_a Np)r_a^2 + 2r_a r_b \cos(k_a Np) - \sin(k_a Np)r_b^2 + \exp(2k_b Np)\sin(k_a Np), \tag{9b}$$

respectively, where we have omitted common real prefactors and wavelength independent terms. The expression for $A(m,\lambda)$ can be obtained from the boundary conditions in the glass-chiral nematic and chiral nematic-glass interface in [8] and in our case reads

$$A(m,\lambda) = \frac{(\lambda/p)f + m}{[(\lambda/p)f + m + n]^2}. \tag{10}$$

It is then possible to calculate the DOS of the chiral nematic structure using Eq. (3). An expression qualitatively similar to Eq. (4) has been previously derived for the transmission coefficient of a FP cavity using the optical transfer function approach [12,13]. The feedback mechanism in chiral nematic LCs, however, differs substantially and lasing in the latter is referred to as "mirrorless." If we consider only the diffracting wave, the eigenfield to which emission is coupled is $E = \exp(ikz)\hat{e}$ (where $\hat{e}$ is the unit polarization vector, which is wavelength dependent) [5,14]. Regarding the sign of the small additive imaginary term to the dielectric constant, $\gamma > 0$ and $\gamma < 0$ correspond to losses and gain, respectively. As we have no prior knowledge to assume otherwise, we assume that the losses, etc., are the same for both the dielectric constants parallel and perpendicular to the director, i.e., $\gamma_\perp = \gamma_\parallel$. This is the case when spontaneous emission is isotropic in terms of polarization and it is perhaps reasonable to assume that the stimulated absorption and emission are also isotropic. A similar approach is also followed in [15], where equal small imaginary parts are added to the ordinary and extraordinary refractive indices of the chiral nematic LC slab in order to account for gain in an active cell and therefore calculate the corresponding transmission coefficient of a defect mode structure.

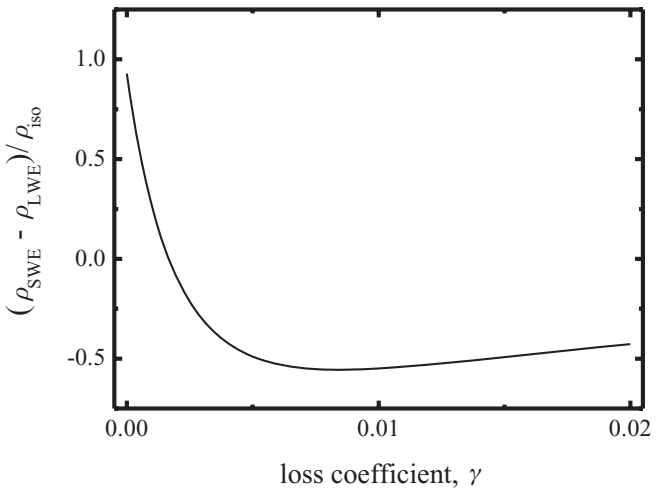

FIG. 2. The asymmetry in the DOS at the first edge modes either side of the photonic band gap of a chiral nematic LC. A plot of the difference of the maximum DOS between the short and long wavelength edges ($\rho_{SWE} - \rho_{LWE}$) of the eigenwave E_1 that is normalized to isotropic DOS as a function of the loss coefficient. In this case $n = 1.581$, the optical anisotropy is $\alpha = 0.1$, and the cell thickness is $L = 30p$.

If we assume an isotropic absorption of the dye we can see directly from Eq. (2) that the relative fluorescent intensities are then only directly proportional to the DOS when the spatial dependence of the normal modes is deemed unimportant in the calculation of the orientational average of the electric dipole moment of the gain medium [5]. On the other hand, one can consider that absorption is characterized by dichroism as in [12,13] because the dye molecules (usually rodlike with a length exceeding that of the liquid crystal molecules) tend to adopt to some extent the local nematic order. However, in our analysis we will not take into account dichroism in the absorption or fluorescence of the gain medium as we will assume an order parameter $S_d \to 0$ pertaining to the case of an isotropic dye. In that case, the relative intensity contributions for each eigenmode are directly proportional to the DOS [Eq. (2)]. When taking into account losses and gain we employ Eq. (4) to calculate the transmission coefficient and then Eq. (3) for the corresponding DOS of the diffracting eigenwave.

Examples of the normalized DOS for the diffracting eigenwave as a function of the reduced wavelength are depicted in Fig. 1 for different values of α and the loss coefficient γ. Figures 1(a) and 1(b) are for the same optical anisotropy but with different magnitudes of the losses. On the other hand, Figs. 1(c) and 1(d) show the profile of the DOS for the same values of the loss coefficient but a smaller optical anisotropy. As can be seen from the plots, the DOS decreases dramatically with increasing losses, regardless of the magnitude of the optical anisotropy, which is a result that can be shown for a FP resonator in the presence of losses [3]. Additionally, the DOS is larger at the band edges for a greater optical anisotropy with the same number of pitches and loss coefficient. In this example, as an order of magnitude increase in the loss coefficient (from $\gamma = 0.0002$ to $\gamma = 0.002$) results in a reduction of the DOS by a factor of 2. The decrease in the DOS has also been noted when an imaginary term is included only in the dielectric constant parallel to the director [3]. In such a case, the short wavelength edge (SWE) is unaffected by the loss factor as

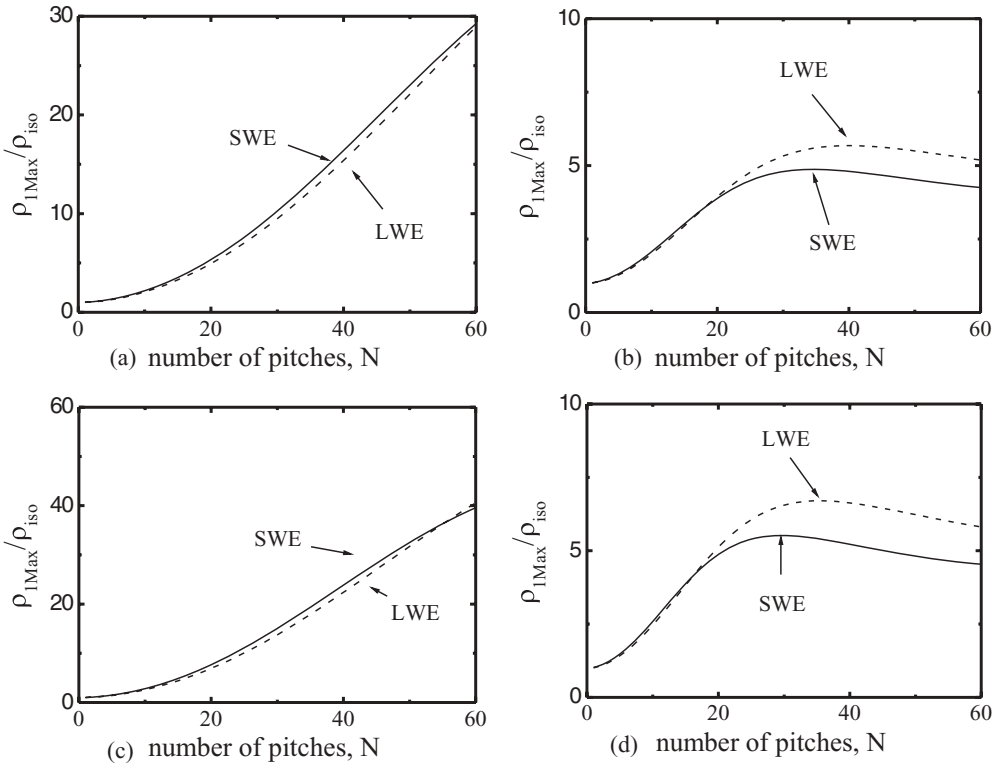

FIG. 3. Theoretical plots of the maximum normalized DOS ($\rho_{1\mathrm{Max}}/\rho_{\mathrm{iso}}$) of the eigenwave E_1 at the two wavelength edges either side of the stop band as a function of the chiral nematic LC. The cell thickness is $L = Np$. (a) For $n = 1.581$, $\alpha = 0.1$ and $\gamma = 2\gamma_{\parallel} = 0.0002$, (b) for $n = 1.581$, $\alpha = 0.1$ and $\gamma = 2\gamma_{\parallel} = 0.006$, (c) for $n = 1.603$, $\alpha = 0.1245$ and $\gamma = 2\gamma_{\parallel} = 0.0002$, and (d) for $n = 1.603$, $\alpha = 0.1245$ and $\gamma = 2\gamma_{\parallel} = 0.006$. The arrows mark the number of pitches where the peak DOS is attained for each wavelength edge. The short wavelength and long wavelength edges are shown as solid and dashed lines, respectively.

opposed to the long wavelength edge (LWE) whose value is diminished.

What is interesting to note is the reversal of the maximum value of the normalized DOS between the SWE and LWE. Unlike the DOS in a quarter-wave stack [10], the DOS profile of a nonabsorbing chiral nematic LC is nonsymmetric with respect to the center of the stop band. Figure 2 shows the ratio of the difference of DOS at the SWE and the LWE to the isotropic DOS as a function of γ. For small values of γ, the maximum value of ρ occurs at the SWE. As γ increases, the difference in ρ at the two edge modes (EMs) approaches zero before the LWE dominates for large losses. Therefore, when choosing the optimum EM for laser emission it is important to consider the losses in addition to the projection of the optical field onto the transition dipole moment of the laser dye.

It should be noted that the profile is symmetric with respect to the center of the stop band occurring at $\lambda' = 1$ for an infinitely thick nonabsorbing cell and that the SWE and LWE are located at $\lambda' = \sqrt{1-\alpha}$ and $\lambda' = \sqrt{1+\alpha}$, respectively [5]. For a finite cell, however, the position of the SWE is displaced towards shorter wavelengths (and the position of the LWE is displaced towards longer wavelengths) [5]. As losses become more dominant, we find that the DOS peaks broaden and are further shifted, in direct analogy with the behavior of the resonance peak in damped steady state oscillating systems.

The variation of the value of the maximum DOS at either wavelength edge for different loss coefficients in cells with varying thickness is considered in Fig. 3. The position of that maximum is found to shift to smaller values of the number of pitches with greater optical anisotropy, which is an indication of enhanced feedback. In particular, in this case we can observe that, when losses are present, the position of the maximum value DOS of the LWE is $L \simeq 40p$ for a cell with optical anisotropy $\alpha = 0.1$ [Fig. 3(b)], which is reduced to the value of $L \simeq 35p$ for a 25% increase in α [Fig. 3(d)]. These results also highlight the interchange between the SWE and LWE as the value of γ is increased. For example, in Fig. 3(a) the SWE exhibits the largest value of ρ for all values shown of the pitch. However, when sufficiently large losses are incorporated, the LWE exhibits the largest DOS for sufficiently large N. The same occurs for a larger optical anisotropy (birefringence) although the maximum DOS is found to be slightly higher. Regarding the variation of the maximum value of the DOS with cell thickness the relation

$$\rho_{\mathrm{Max}} \propto L^2 \exp(-\beta L) \tag{11}$$

has previously been proposed to pertain to the experimental data of the energy-excitation threshold of cells as a function of N with $L = Np$ being the length of the cell and β the collective absorption coefficient [3]. The general trend suggested by Eq. (11) is indeed vindicated by our theoretical findings: the deviation from the parabolic profile is more ostensible with increasing losses and a maximum is observed whose position and value depend on both the loss coefficient and the optical anisotropy. The parabolic dependence of the DOS at

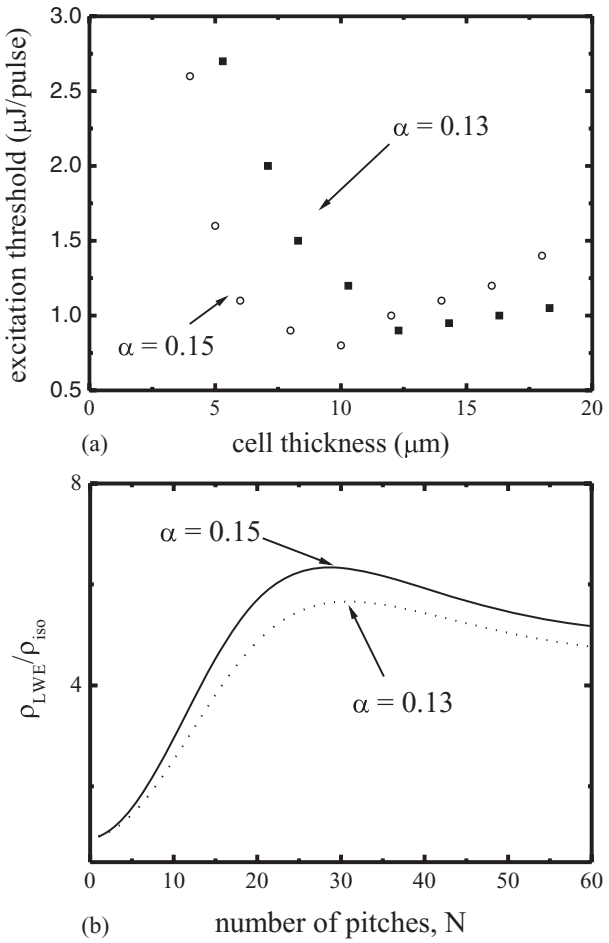

FIG. 4. (a) Experimental results of the dependence of the laser excitation threshold on the cell thickness for a low optical anisotropy ($\alpha = 0.13$) (closed squares) and a high optical anisotropy ($\alpha = 0.15$) (open circles) LC host. (b) Theoretical plots of the DOS for the long wavelength band edge for two different chiral nematic LCs for the same optical anisotropies as those used in the experiment. The loss coefficient in this case is $\gamma = 0.0084$ for $n = 1.608$ and $n = 1.627$, respectively.

the wavelength of the photonic band edges is a well known result for quarter wave stacks [10] as well as for nonabsorbing chiral nematic LCs [3].

Experimentally, the dependence of the DOS upon the number of pitches for different optical anisotropies is verified, albeit indirectly, by determining the excitation threshold as a function of cell thickness, Fig. 4(a). As shown in Eq. (1) the excitation threshold is inversely proportional to ρ. The figure shows the excitation threshold as a function of the cell thickness for two different LC laser samples. These measurements were obtained using two different laser samples: one consisting of the nematic LC $E7$ ($\alpha = 0.13$ and $\Delta n = 0.2$ at 25 °C) and the other with the nematic LC mixture $E49$ ($\alpha = 0.15$ and $\Delta n = 0.25$ at 25 °C). The optical anisotropies were determined from the refractive indices parallel and perpendicular to the director of the nematic sample at a fixed wavelength of 589.6 nm using an Abbe refractometer. Both mixtures were doped with a high twisting power chiral dopant (BDH1281, Merck KGaA) and the laser dye DCM (Exciton). The samples were capillary filled into wedge cells that were fabricated in-house and were coated with a rubbed polyimide alignment layer to ensure that a Grandjean texture was obtained after filling. Each cell was optically excited by the second harmonic of an Nd:YAG laser (Polaris II, New Wave Research) at positions within the wedge cell for which the dimensions of the cell gap were known. In both cases the emission wavelength and the pitch ($p \approx 350$ nm) were the same but the main difference was the optical anisotropy of the nematic host. The profile of the plot resembles the inverse of the dependence of the DOS on the number of pitches confined within the device (cf., Fig. 3) as suggested in Eq. (1). The minimum in the excitation threshold is found to occur at smaller cell thicknesses (corresponding to a smaller N required for the maximum value of the DOS) for the higher optical anisotropy compound ($E49$) than that obtained for the laser sample with a lower optical anisotropy ($E7$). In this case, the minimum excitation threshold is found to occur at $L = 12.5\,\mu$m for the sample consisting of $E7$ ($\alpha = 0.13$) and is shifted to $L = 10\,\mu$m when the LC host is replaced with $E49$ ($\alpha = 0.15$). For the purposes of comparison, theoretical curves for the DOS for two different samples with the same optical anisotropy as $E7$ and $E49$ are shown in Fig. 4(b) for a suggested value of $\gamma = 0.0084$. Theoretically, we find that the number of pitches required to obtain the maximum DOS for the higher optical anisotropy sample is reduced from $N = 32$ to $N = 28$, which is in good agreement with the experimental results whereby the difference in the number of pitches for the two lasers is found to be $\Delta N \approx 5$.

We will now take into consideration the gain of the active material in the process of laser emission. For an amplifying medium with $\gamma < 0$ we find that the DOS of various EMs diverges at particular values of γ, which are the lasing excitation gain coefficients for these modes. The behavior is consistent with the case of an active medium filling a FP resonator, where the DOS diverges at threshold [5]. In Fig. 5 we depict the DOS of an amplifying chiral nematic LC for different values ofγ. For $|\gamma| \ll 1$ and for sufficiently thick cells, the threshold gain coefficient $\gamma_{\rm th}/n^2$ is found to be inversely proportional to α^2 as well as to L^3 [3,11]. As the threshold value for a chiral nematic LC with a given thickness is approached, the DOS rapidly diverges suggesting a theoretically infinite group time of photons residing in the resonating cavity. In actuality, the DOS does not reach infinity due to the finite lifetime of the excited state or due to the collision with a phonon [13,16]. Its value depends on the microscopic properties of the sample and the duration of the pumping. If the gain factor exceeds slightly the threshold value, the DOS is still very high and the phase derivative changes sign [13]. Such a sign reversal is depicted in Fig. 5(b) where the magnitude of the gain coefficient exceeds the value satisfying the exact lasing condition for the SWE mode. These values of γ belong to the regime of "superamplification" [13]. As the gain coefficient is further increased the EM that first attained threshold (in one of the wavelength edges) is now quenched and laser action is triggered for successive EMs [Fig. 5(c)]. We should also note here that, apparently, only the absolute value of the DOS depicted in these graphs is physically meaningful when referring to Fermi's golden rule in Eq. (2). In accordance with the remarks of the author in [12], the region of

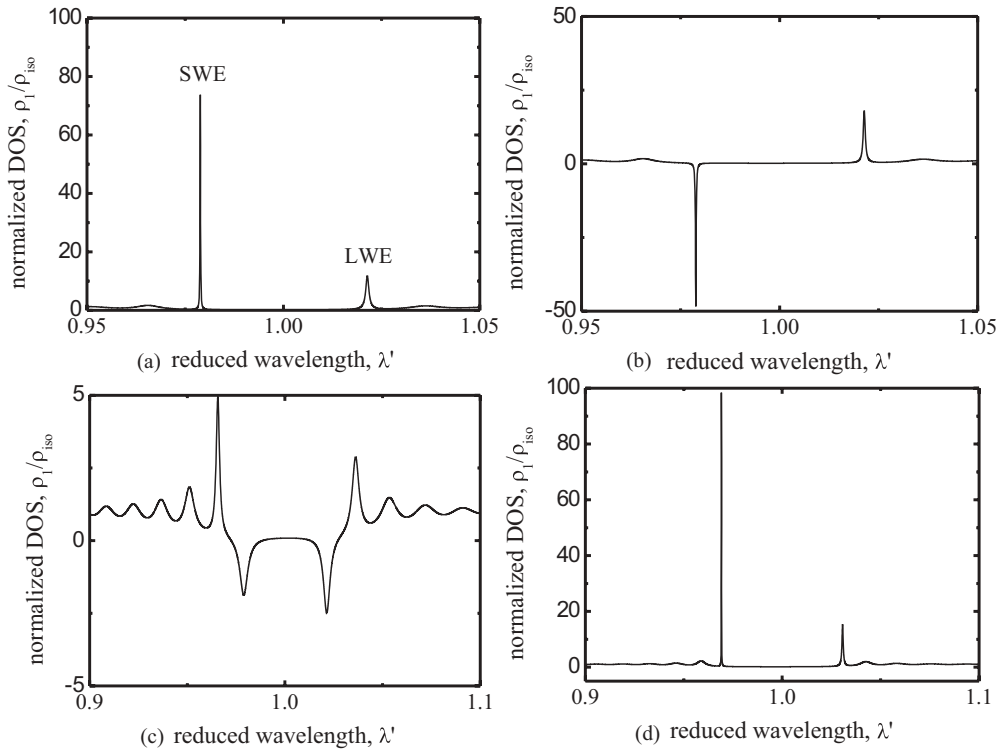

FIG. 5. The behavior of the DOS in the presence of gain. Normalized DOS of the eigenwave E_1 for a chiral nematic LC cell with thickness $L = 30p$. $n = 1.523$, $\alpha = 0.03$ and (a) $\gamma = 2\gamma_{\parallel} = -0.0304$, (b) $\gamma = 2\gamma_{\parallel} = -0.0320$, (c) $\gamma = 2\gamma_{\parallel} = -0.0540$, (d) $n = 1.541$, $\alpha = 0.0526$ and $\gamma = 2\gamma_{\parallel} = -0.0134$.

superamplification does not only correspond to the case where losses are slightly higher than the active medium gain but also to the case in which they are marginally overcompensated. That behavior can be traced also in the transmission and reflection coefficients in the region of anomalous absorption for amplifying chiral nematic LCs and other DFB structures [11,16].

Our results are in good agreement with the behavior of the threshold values obtained from the maximization of transmittance and the solvability condition of the system produced by satisfying the continuity conditions of tangential electric field components in a boundary value problem formulation for light propagation in chiral nematic LCs [11]. As we also observe in Fig. 5(d), a smaller gain constant is required for the DOS of the lasing mode to diverge in a chiral nematic LC with greater birefringence, which is an indication of enhanced feedback. Once the threshold gain has been identified, it can be directly linked to the critical population inversion $\Delta N_{\text{th}}^{\text{e}}$ via [16]

$$\gamma_{\text{th}} \propto g_{\text{th}} = \Delta N_{\text{th}}^{\text{e}} \frac{\lambda^2}{8\pi n'^2 \tau_{\text{sp}}} g(\omega), \omega = 2\pi c/\lambda, \qquad (12)$$

where $g(\omega)$ is the linewidth function, n' is the refractive index of the medium away from resonance, and τ_{sp} is the spontaneous lifetime of the transition. For dye-doped cells, the population inversion is equal to threshold gain divided by the molecular cross section for spontaneous emission, which is experimentally determined from the luminescence spectrum (under low pumping) of the fluorescent dyes normalized to the ratio $\Phi/(8\tau_{\text{sp}})$, where Φ is the fluorescence quantum yield [7].

Moreover, the experimentally determined emission spectral width (full width at half maximum) $\Delta\omega$ of both fluorescence and lasing can be directly related to the DOS via the uncertainty principle [13]

$$\Delta\tau \cdot \Delta\omega \propto \pi, \qquad (13)$$

bearing in mind that the DOS is linked to the characteristic time $\Delta\tau$ as [13,17]

$$\rho = \frac{\Delta\tau}{L} \propto \frac{\pi}{L\Delta\omega}. \qquad (14)$$

In conclusion, we have derived analytic expressions for the calculation of the density of photon states (DOS) in dye-doped chiral nematic cells in the presence of an active lossy medium. Results are presented on the profile of the DOS as a function of the reduced wavelength for different macroscopic parameters such as the optical anisotropy and the magnitude of the losses. The results show that, for a fixed value of the pitch, the DOS at the photonic band edges decreases with increasing losses. The band edge that exhibits the largest DOS (e.g., short or long wavelength band edge) is found to depend on the magnitude of the loss coefficient; above a critical value the long wavelength edge exhibits the largest DOS. Using the analytical expressions, results have been presented on the DOS as a function of the number of pitches showing an optimal value of the pitch that corresponds to the maximum in the density of states. These findings are correlated with experimental results for the lasing threshold, which is found to be inversely proportional to the maximum DOS when only

losses are considered (apart from stimulated absorption). The behavior of the DOS can also reflect mode quenching in these lasing structures in the regime beyond the threshold gain. It is understood that the consideration of the DOS proves to be an invaluable means for understanding lasing and such an approach should be implemented when determining the factors limiting the lasing threshold in chiral nematic films (e.g., leaky modes) as well as when studying the mode behavior in more complicated configurations (e.g., defect modes).

ACKNOWLEDGMENTS

The authors gratefully acknowledge the Engineering and Physical Sciences Research Council (UK) for financial support through the COSMOS research project (EP/H046658/1) and the Photonics Systems Centre for Doctoral Training. One of the authors (S.M.M.) gratefully acknowledges The Royal Society for financial support. One of the authors (T.K.M.) gratefully acknowledges the Onassis Foundation for financial support.

[1] I. P. Il' chishin, E. A. Tikhonov, V. G. Tishchenko, and M. T. Shpak, JETP Lett. **32**, 24 (1980).
[2] For a recent review, see H. J. Coles and S. M. Morris, Nature Photonics **4**, 676 (2010).
[3] M. F. Moreira, S. Relaix, W. Cao, B. Taheri, and P. Palffy-Muhoray, *Liquid Crystal Microlasers* (Transworld Research Network, Kerala, India, 2010), Chap. 12, p. 223.
[4] C. Mowatt, S. M. Morris, T. D. Wilkinson, and H. J. Coles, Appl. Phys. Lett. **97**, 251109 (2010).
[5] J. Schmidtke and W. Stille, Eur. Phys. J. B **31**, 179 (2003).
[6] S. M. Morris, A. D. Ford, G. Gillepsie, M. N. Pivnenko, O. Hadeler, and H. J. Coles, J. Soc. Info. Disp. **14**, 565 (2006).
[7] L. M. Blinov, JETP Lett. **90**, 166 (2009).
[8] Hl. de Vries, Acta Crystallogr. **4**, 219 (1951).
[9] M. D. Tocci, M. Scalora, M. J. Bloemer, J. P. Dowling, and C. M. Bowden, Phys. Rev. A **53**, 2799 (1996).
[10] J. M. Bendickson, J. P. Dowling, and M. Scalora, Phys. Rev. E **53**, 4107 (1996).
[11] V. A. Belyakov and S. V. Semenov, JETP **109**, 687 (2009).
[12] S. P. Palto, JETP **103**, 472 (2006).
[13] S. P. Palto, *Liquid Crystal Microlasers* (Ref. [3]), Chap. 8, p. 141.
[14] As explained in [8] the sign of the wave vector must change in the region $\lambda' > \sqrt{1+\alpha}$ for the Poynting vector to be in the correct direction. This is inconsequential for the calculation of the transmission coefficient and the DOS.
[15] Y. Zhou, Y. Huang, Z. Ge, L.-P. Chen, Q. Hong, T. X. Wu, and S.-T. Wu, Phys. Rev. E **74**, 061705 (2006).
[16] A. Yariv and P. Yeh, *Photonics: Optical Electronics in Modern Communications*, 6th ed., (Oxford University Press, Oxford, 2007).
[17] S. P. Palto, L. M. Blinov, M. I. Barnik, V. V. Lazarev, B. A. Umanskii, and N. M. Shtykov, Crystallogr. Rep+. **56**, 622 (2011).